Molecular Diversity
https://doi.org/10.1007/s11030-021-10368-3

ORIGINAL ARTICLE

An efficient and green one-pot synthesis of tetrahydrobenzo[a]xanthenes, 1,8-dioxo-octahydroxanthenes and dibenzo[a,j]xanthenes by Fe_3O_4@Agar-Ag as nanocatalyst

Kimia Hoseinzade[1] · Seyed Ali Mousavi-Mashhadi[1] · Ali Shiri[1]

Received: 31 October 2021 / Accepted: 13 December 2021

Abstract
Agar-coated Fe_3O_4 nanoparticles (Fe_3O_4@agar) were prepared simply through in situ co-precipitation of Fe^{2+} and Fe^{3+} ions via NH_4OH in an aqueous solution of Agar. Coating of Ag^+ ions on the surface of the latter followed by mild reduction of Ag^+ with $NaBH_4$ gives Fe_3O_4@Agar-Ag NPs. The magnetic Fe_3O_4@Agar-Ag nanocatalyst was characterized thoroughly by FT-IR, XRD, SEM, TEM, VSM, EDX, TGA, and ICP analyses. Its catalytic activity was assessed in the synthesis of 12-aryl-8,9,10,12-tetrahydrobenzo[a]xanthene-11-one, 14-aryl-14*H*-dibenzo[a,j]xanthenes, and 1,8-dioxo-octahydroxanthene derivatives through a one-pot condensation of dimedone, 2-naphthol, and aryl aldehydes in EtOH. This novel method represents lots of advantages compared to the previous researches, such as avoiding the toxic catalysts, easy method for isolation of the products, satisfying yields, totally clean conditions, and simplicity of the methodology. This catalytic system is attributed to an eco-friendly process, high catalytic activity, and facility of recovery using an external magnet.

Graphical abstract

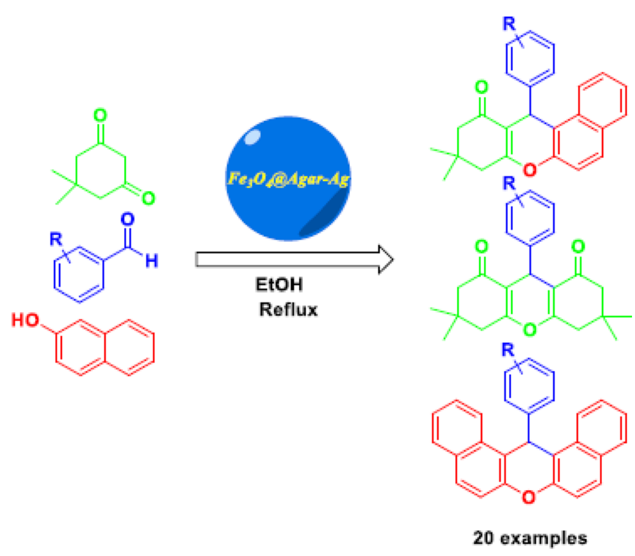

A novel and magnetically recyclable catalyst known as Fe3O4@Agar-Ag NPs as a heterogeneous catalyst were synthesized by a simple method. Using this facile, efficient, and eco-friendly Nanocomposite, for the different models of xanthene reaction was represented.

Keywords Nanoparticles · Heterogeneous catalyst · Xanthenes · One-pot reaction

Extended author information available on the last page of the article

Published online: 29 January 2022

Introduction

In recent decades, multicomponent reactions had a special place in the synthesis of chemical compounds for researchers and scientists, since they can display a wide range of exciting properties [1–5]. Xanthene derivatives are considered in biological resources such as antitumor, antiviral, anti-inflammatory, florescence-ratio spectroscopy, and therefore, they are considered as high priority structures [6–11]. For instance, the *Gartanin* compound (Fig. 1A) showed significant antioxidant activity.[12] Besides, due to their useful spectroscopic properties, such compounds are also a natural source of xanthene dyes, for example, *Rhodomyrtone* (Fig. 1B) extracted from *Rhodomyrtus tomentosa* and a compound known as BF6 (Fig. 1C) extracted from the leaves of *Baeckea frutescens* are natural xanthene diones with many features [8, 13, 14].

Due to their perfect range of applications and properties of xanthene derivatives, the discovery of a new and efficient catalyst with high catalytic activity, recyclability, and simple reaction working-up for the preparation is of prime interest. Lots of catalysts have been represented for the synthesis of xanthene reactions such as ($H_4SiW_{12}O_{40}$) [15], ($H_5PW_{10}V_2O_{40}$/MCM-48) [16], ($HClO_4$–SiO_2 and PPA–SiO_2) [17] and (Triethylaminium-N-sulfonic acid trifluoroacetate {[TEASA][TFA]}) [18]. However, these catalysts have many limitations, such as strong acidic conditions, long reaction times, low yields, and harsh reaction conditions [19–21]. To avoid these limitations, a recyclable, non-toxic, and easily prepared catalyst can be considered as a highly effective method, and the catalyst is also totally recoverable from the reaction mixture by using an external magnet [22–26]. Magnetic nanoparticles are popular for special crafty usage in biotechnology, health and environment, material science, and catalysis. The surface of MNPs is typically modified or coated with renewable and different polymers and metals to improve their colloidal stability and surface functionalization capability [27–34].

Many polymers can provide excellent system in the form of coating magnetic nanoparticles and making a stable network structure [35–37]. Specifically, an increasing consideration has been recently focused on the synthesis of Agar coated Fe_3O_4 NPs [38–40]. Agar resides in the cell wall of red algae, and it is composed of a strongly gelling seaweed hydrocolloid and commonly used in food industry. As an ideal support material, Agar has its particular properties inclusive of availability, safety, biocompatibility, biodegradability, low immunogenicity, and antibacterial properties, and also, it is used as non-toxic and non-expensive linker [41–44]. Organic synthesis catalyzed by metals is extremely developed [45–47]. Silver is known as a soft, white, transition metal, and it exhibits the highest electrical conductivity and thermal conductivity [48]. Ag NPs are appropriate for their properties as substrates in catalysis studies, surface incensement, and the biomedical fields [49]. Polymer coated metal nanoparticles are known for high surface area, highly available, non-toxic, and stability of pH during the reaction.

However, in continuation of our previous works[50–56], now we introduce a simple, low cost, highly- effective, non-toxic, and new catalytic system for the synthesis of xanthene derivatives from one-pot condensation of 2-naphthol, dimedone (5,5-dimethyl-1,3-cyclohexanedione), and different aldehydes with different random products using Fe_3O_4@Agar-Ag NPs catalyst in ethanol as an eco-friendly solvent (Schemes 1, 2).

Results and discussion

The preparation and characterization of the Fe_3O_4@Agar-Ag catalyst

Initially, in order to synthesize novel catalysts and develop the practically and environmentally good methodologies for the organic reactions, the structure of Fe_3O_4@Agar-Ag is identified and characterized by different analyses, including Fourier transform infrared (FT-IR), X-ray diffraction (XRD), scanning electron microscopy (SEM), transmission electron microscopy (TEM), vibrating sample magnetometry (VSM), energy dispersive X-ray (EDX), thermogravimetric (TGA), and inductively coupled plasma (ICP) analyses.

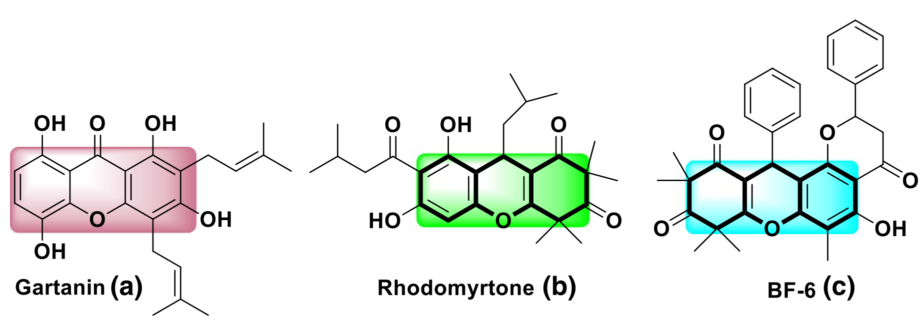

Fig. 1 Examples of xanthenes in natural compounds

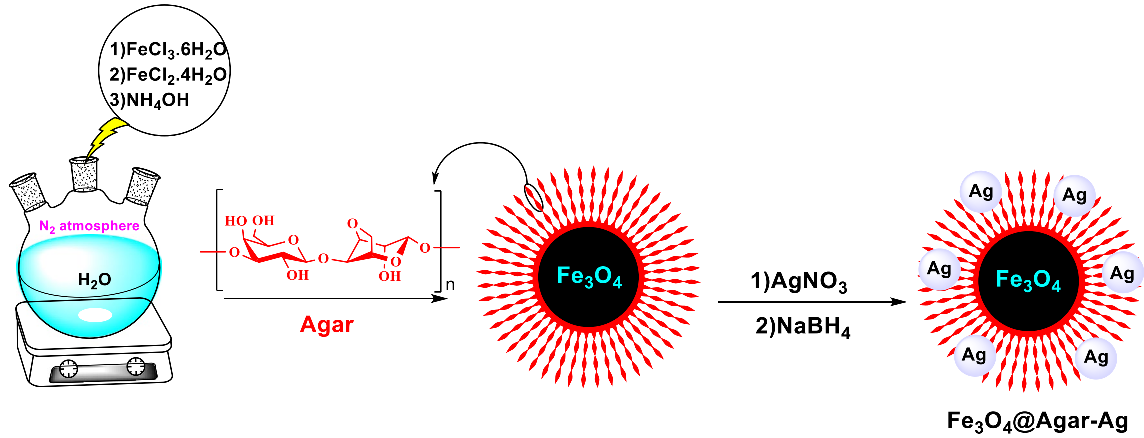

Scheme 1 Synthesis of Fe_3O_4@Agar-Ag NPs catalyst

Scheme 2 General procedure for the synthesis of xanthene derivatives

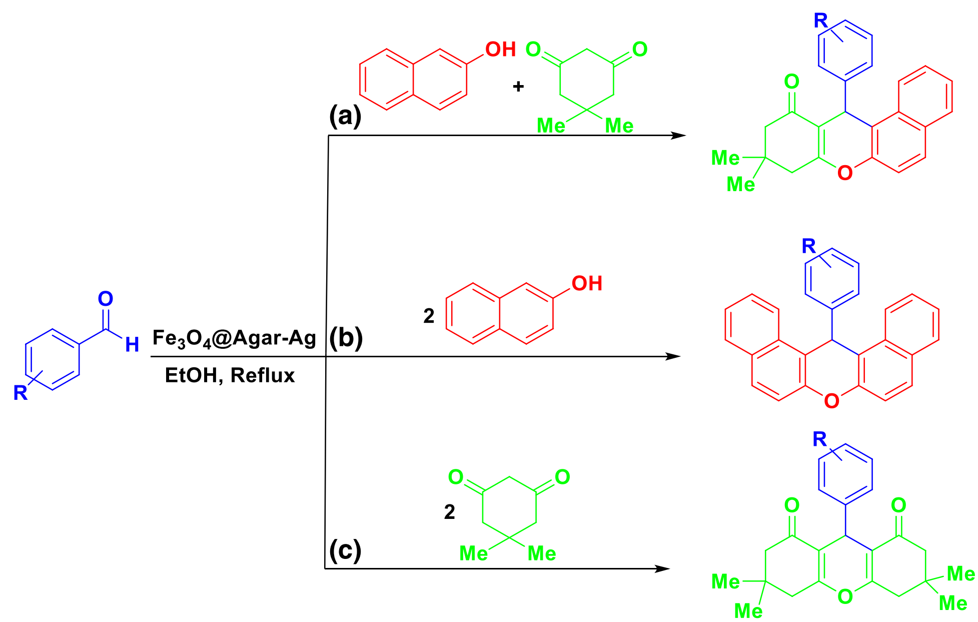

In Fig. 2, the FT-IR spectrum demonstrated the C–O absorption of Agar at 1060 cm^{-1} along with a peak at 598 cm^{-1} related to the stretching vibration of the Fe–O bond group in Fe_3O_4@Agar. This exhibits that magnetic Fe_3O_4 NPs have been coated by Agar. Conceivable bindings of silver with OH group in Fe_3O_4@Agar-Ag NPs have been ascribed to the combined intensity of hydroxyl peaks at 3435 cm^{-1}. Rupture of the bending bands of hydroxyl at 1622 cm^{-1} and 1346 cm^{-1} also detects the bonding of Ag with OH groups. The differences in the area of 1400 cm^{-1} and 1000 cm^{-1} are associated to the perturbation in C–O vibrations induced by Agar-Ag complexation (Fig. 2).

The XRD patterns help to study the crystallinity of the catalyst, Fe_3O_4@Agar NPs, and Fe_3O_4@Agar-Ag NPs. According to standard pattern COD Card Number [96-900-2328] and [96-500-0219], which indicate the pure crystalline structures of Fe_3O_4 and silver, the sharp peaks confirm the excellent crystallinity of the prepared samples (Fig. 3). For Fe_3O_4@Agar NPs, the outcome is in accord with the standard patterns of inverted cubic spinel magnetite (Fe_3O_4) crystal structure. It shows six diffraction peaks at 2θ about 30.8°, 38.0°, 54.8°, 58.0°, 64.3°, and 77.3° marked by their corresponding indices (2 0 2), (3 1 1), (2 2 2), (3 3 3), (4 0 4), and (5 3 3), respectively. The small and weak broad bands in the range of 20°–27° detect the existence of Agar. Diffraction patterns of the Fe_3O_4@Agar-Ag NPs demonstrate three additional peaks at 2θ about 38.0°, 44.2°, and 77.3°; corresponding to (1 1 1), (2 0 0), and (3 1 1) planes of face-centered cubic (fcc) silver crystal structure. No impurities in the XRD patterns infer the formation of net Fe_3O_4 and Ag nanoparticles.

Fig. 2 FT-IR spectrum of **a** Agar, **b** Fe_3O_4@Agar NPs, **c** Fe_3O_4@Agar-Ag NPs, and **d** Recycled catalyst

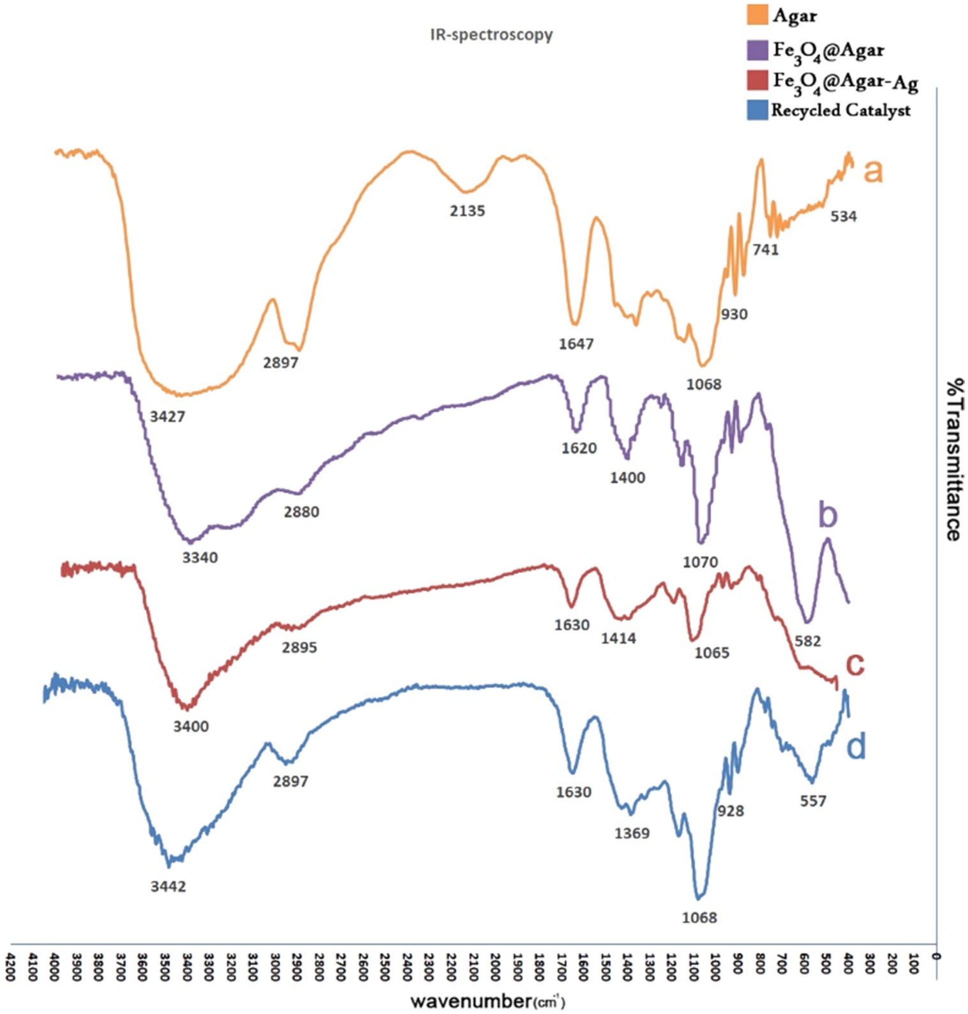

Fig. 3 X-ray diffraction spectroscopy for Fe_3O_4@Agar-Ag NPs

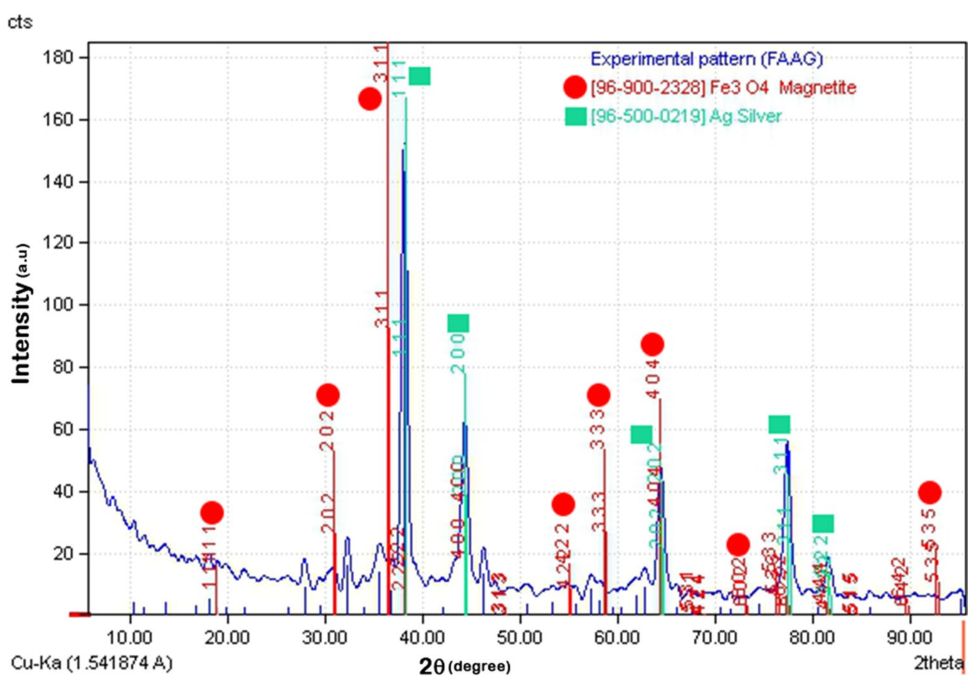

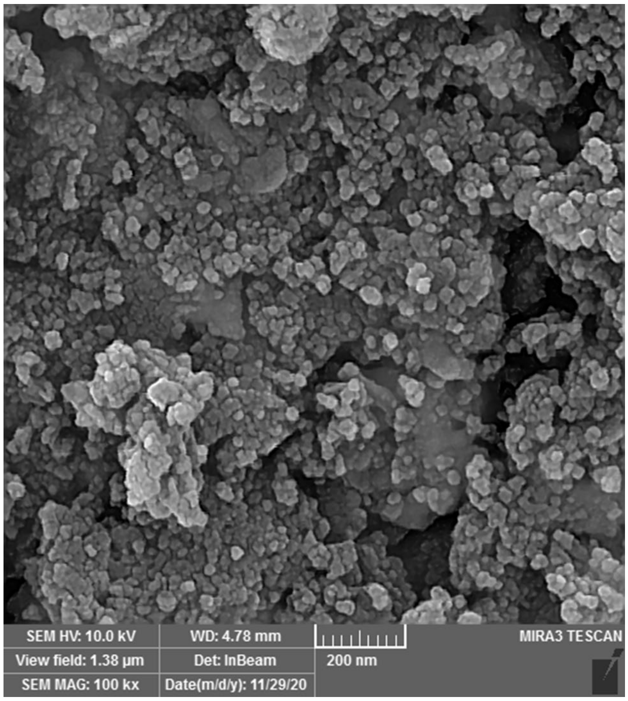

Fig. 4 Scanning electron microscopy (SEM) for Fe_3O_4@Agar-Ag NPs at 200 nm

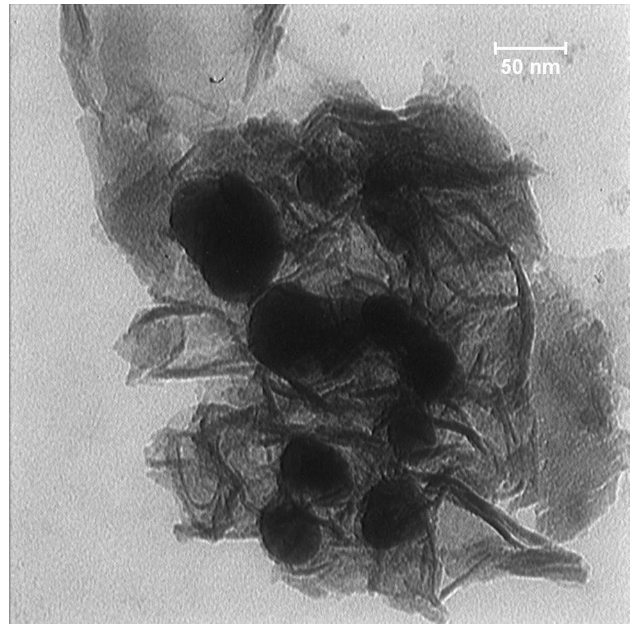

Fig. 5 Transmission electron microscopy (TEM) for Fe_3O_4@Agar-Ag NPs at 50 nm

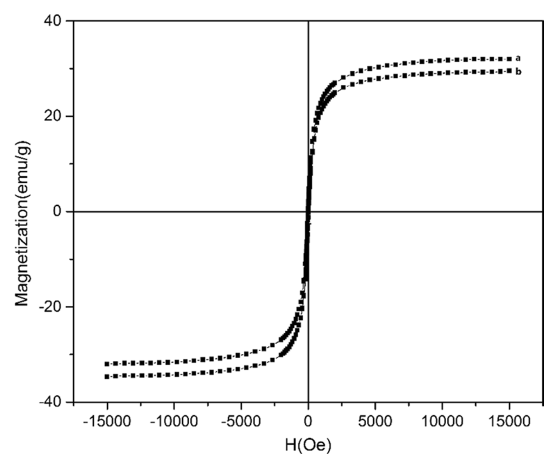

Fig. 6 Vibrating-sample magnetometer (VSM) spectroscopy **a** Fe_3O_4@Agar and **b** Fe_3O_4@Agar-Ag NPs

The FE–SEM image showed that the nanoparticles were still almost nanospherical in its 3D form with nanometer-sized particles of less than 25 nm in diameter. Figure 4 shows the morphology of the Fe_3O_4@Agar-Ag nanoparticles with a core–shell structure. However, it is presumed that this particle size causes the catalyst to be more in touch with the reactants, which leads to a good yield of the desired product**.**

TEM image of the catalyst displayed in Fig. 5. The circular form of any nanoparticle corresponded to the core of the catalyst, similar to the FE-SEM image that can be observed at a scale of less than 25 nm. Also, TEM images show that magnetic nanoparticles of Fe_3O_4 have been surrounded by the biopolymeric network of Agar. Some gathering of particles was also observed in the TEM image. It is proposed that this accumulate is due to the entrapment of the particles in the hollow pore structure of the agar gels.

The magnetic properties of nanoparticles have been measured with a vibrating sample magnetometer for Fe_3O_4@Agar (Fig. 6a) and Fe_3O_4@Agar-Ag (Fig. 6b) NPs. They were constructed in the limited area of − 15,000–15,000 Oe using VSM. As shown in Fig. 6, the impregnation magnetization of Fe_3O_4@Agar-Ag NPs is 35 emu g^{-1}, lower than that of Fe_3O_4@Agar (33 emu g^{-1}). The magnetization diagram displays that the Fe_3O_4@Agar-Ag NPs have paramagnetic properties in which the nanoparticles can be easily separated from the reaction melange using an external magnet.

Elemental compositions were determined with EDX analysis for Fe_3O_4@Agar-Ag NPs (Fig. 7). The EDX pattern supports the excellent dispersion of Fe_3O_4@Agar-Ag NPs. Chemical characterization of the nanoparticles showed that iron, carbon, oxygen, and silver elements are involved. This analysis also detected the presence of 11.11 mol% Ag in Fe_3O_4@Agar-Ag NPs.

TGA of Fe_3O_4@Agar-Ag NPs was manipulated in the confine of 25–550 °C (Fig. 8). The first mass loss of Fe_3O_4@Agar-Ag NPs at below 140 °C is due to the removal of physically adsorbed water. The second and the significant weight

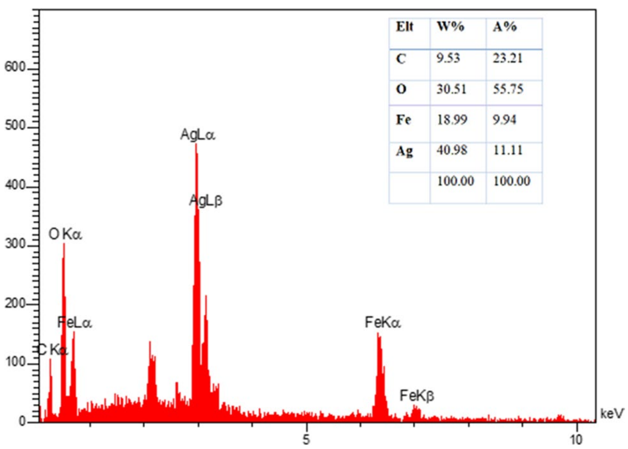

Fig. 7 Energy-dispersive X-ray spectroscopy for Fe_3O_4@Agar-Ag NPs

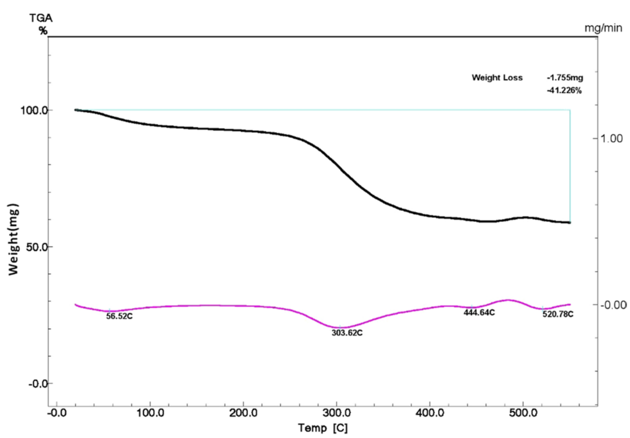

Fig. 8 Thermogravimetric analysis of Fe_3O_4@Agar-Ag NPs

loss (−41.226%) of Fe_3O_4@Agar-Ag NPs in the range of 210–460 °C is attributed to Agar as the organic moiety.

In order to determine the optimization of the reaction conditions such as solvent, amount of catalyst, and temperature, benzaldehyde is selected in the model reactions, and the results will be represented in Table 1.

According to Table 1, the model reaction was studied by examining the various amounts of the catalyst. The efficiency of the catalyst activity with different amounts involving 0, 5, 10, 15, 20, 25, and 30 mmol% of Fe_3O_4@Agar-Ag NPs was studied. The results demonstrated no or trace product observed in the absence of the catalyst or catalyst without metal. 20 mmol% showed the optimum amounts of the catalyst in which the increasing of this amount did not show any significant effect. We also tested the result of different temperatures and solvents such as DMSO, EtOH, DMF, and H_2O. The product yields increase at reflux condition with EtOH as solvent.

The reaction of various aldehydes with three model reactions resulted in satisfied yields (Table 2). The first model is the general reaction for xanthene using aldehyde (1 mmol), 5,5-dimethyl-1,3-cyclohexanedione (1 mmol), and 2-naphthol (1 mmol) at reflux condition and using ethanol as solvent. The second model reaction contains aldehyde (1 mmol) and 2-naphthol (2 mmol) at the same conditions as the first model, and the third model reaction also contains aldehyde (1 mmol) and 5,5-dimethyl-1,3-cyclohexanedione (2 mmol) with the same condition. Aromatic aldehydes containing electron-donating groups such as methyl, methoxy, and hydroxyl required longer reaction times (10 h), while aromatic aldehydes containing electron-withdrawing groups such as chloro- or nitro-moiety required shorter reaction times (6 h). However, all these three model reactions catalyzed by Fe_3O_4@Agar-Ag NPs represent a selective and mild method with satisfying yields of products.

According to the literature, a plausible mechanism for the synthesis of xanthene reaction for three models of reaction is proposed. [66] (Fig. 9).

To investigate the reusability and leaching of the catalyst, the catalyst removed by an external magnet at the end of the reaction, washed with water, and ethanol, successively. According to the obtained results, the catalyst could maintain its catalytic properties up to six times, and no significant loss in the yield of the products as well as low Ag leaching was observed. (Fig. 10).

The hot filtration test of the catalyst was performed to determine the efficiency of the catalyst. The catalyst particles removed from the reaction by an external magnet after 2.5 h (50% yield). A reaction monitoring using TLC indicated that practically the reaction rate decreased significantly after hot filtration. (Fig. 11).

Later on, to check the performance of the catalyst, we have compared the activity of our catalyst with other reported ones. Table 3 shows the comparison of the reported catalysts that contain limitations and preparation difficulties. It is clear from Table 3 that the current method is simpler, more efficient and exhibited higher yields for the synthesis of xanthene derivatives than the other ones.

Conclusions

In conclusion, a novel and magnetically recyclable catalyst known as Fe_3O_4@Agar-Ag NPs as a heterogeneous catalyst was synthesized by a simple method. Using this facile, efficient, and eco-friendly nanocomposite, for the different models of xanthene reaction was represented. The correct and accurate synthesis of the catalyst was characterized by different analyses. We have exhibited for the first time the use of Fe_3O_4@Agar-Ag NPs as a highly active and efficient

Table 1 The optimization of the model reaction conditions

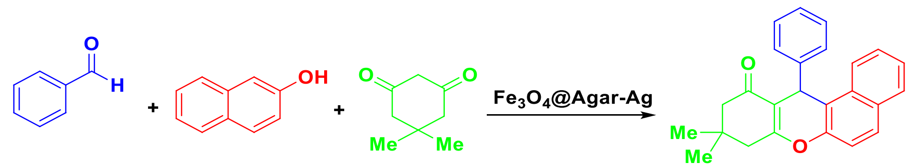

Entry	Catalyst (mmol%)	Temperature (°C)	solvent	Time (h)	Yield (%)
1	0[a]	110	DMSO	15	0
2	5[a]	110	DMSO	15	40
3	10[a]	80	water	15	57
4	15[a]	100	DMF	15	68
5	20[a]	120	DMF	12	80
6	**20[a]**	**Reflux**	**Ethanol**	**6**	**97**
7	25[a]	Reflux	Ethanol	6	96
8	25[a]	110	DMSO	10	87
9	30[a]	Reflux	Ethanol	10	90
10	20[b]	Reflux	Ethanol	20	35
11	20[c]	Reflux	Ethanol	20	40
12	20[d]	Reflux	Ethanol	20	58

Bold indicates theoptimized reaction conditions

[a]Catalyst: Fe_3O_4@Agar-Ag NPs

[b]Catalyst: Fe_3O_4@Agar NPs

[c]Catalyst: Fe_3O_4 NPs

[d]Catalyst: Ag

nanocatalyst for the synthesis of xanthene derivatives via a one-pot reaction in an environmentally friendly solvent.

Experimental

Preparation of Agar-coated magnetic nanoparticles: Fe_3O_4@Agar NPs

A mixture of $FeCl_3.6H_2O$ (6.5 mmol, 1.76 g) and $FeCl_2.4H_2O$ (3.3 mmol, 0.65 g) dissolved in deionized water (120 ml) under intensive and vigorously stirring. Then, NH_4OH solution (25% w/w, 8 ml) was added to the mixture and stirred for 3 h at room temperature. Then, the solution of Agar (1 g) in water (50 ml) was added dropwise. The mixture stirred for 5 h at 70 °C under N_2 atmosphere. The obtained magnetize mixture was separated using magnetic decantation and washed with deionized water (2 × 30 ml), and dried at 50 °C for 24 h.

Synthesis of silver nanoparticles coated magnetic Agar: Fe_3O_4@Agar-Ag NPs

Moreover, $AgNO_3$ solution (80 gr. L^{-1}) was added dropwise over a period of 30 min at room temperature. The mixture was stirred for extra 3 h. Then, $NaBH_4$ was added to the mixture gently within 4 h with stirring. Fe_3O_4@Agar-Ag was obtained by washing with water several times and drying in a vacuum desiccator at room temperature.

General procedure for the synthesis of 12–aryl–8,9,10,12–tetrahydrobenzo[a]xanthene–11–ones derivatives

A mixture of aromatic aldehyde (1.0 mmol), β-naphthol (1.0 mmol), 5,5-dimethyl-1,3-cyclohexanedione (1.0 mmol) and Fe_3O_4@Agar-Ag NPs (20 mmol%) in EtOH (2 mL) was stirred in an oil bath at reflux conditions. The progress of the reaction was monitored by TLC, and after the completion of the reaction, the catalyst was separated from the mixture using an external magnet. The resulting solid was filtered off and recrystallized by ethanol. The catalyst was washed several times with ethyl acetate and ethanol, and dried in a vacuum desiccator to reuse for the next reaction.

9,9-Dimethyl-12-phenyl-8,9,10,12-tetrahydro-11H-benzo[a]xanthen-11-one (1):

Yield = 97%, ^1H NMR (300 Hz, $CDCl_3$): δ (ppm) 1.01, 1.16 (6H, s, CH_3), 2.25–2.39 (2H, m, CH_2), 2.61 (2H, s, CH_2), 5.76 (1H, s, CH), 7.09–7.50 (8H, m, CH), 7.09–8.05 (11H,

Table 2 (a) The reaction of xanthene using aldehyde(1 mmol), dimedone(1 mmol), and 2-naphthol(1 mmol), (b) The reaction for xanthene using aldehyde(1 mmol) and 2-naphthol(2 mmol), (c) The reaction for xanthene using aldehyde(1 mmol) and dimedone(2 mmol)

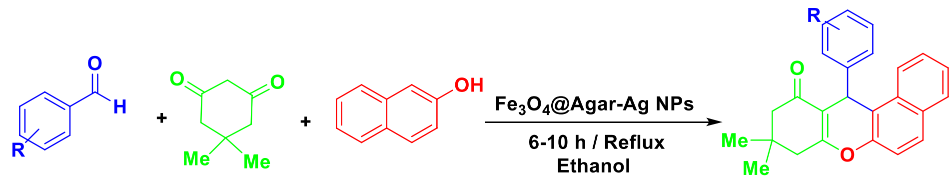

Entry	Aldehyde	Product	Yield (%) /Time (h)	TON	TOF (h^{-1})	Mp (found) °C	Mp (Lit.) °C
1	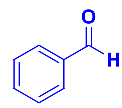	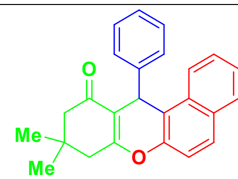 1	97/6	4.85	0.80	(144 –148)	(153–155)[19]
2	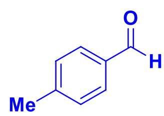	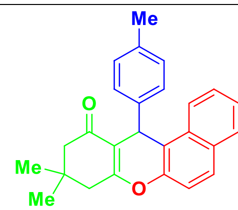 2	90/7	4.5	0.65	(190 –194)	(191–193)[58]
3	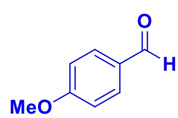	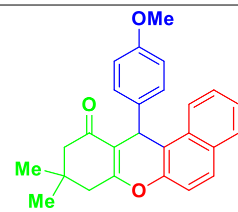 3	87/10	4.35	0.43	(203 –205)	(205–207)[19]
4	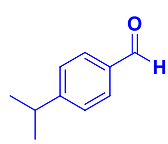	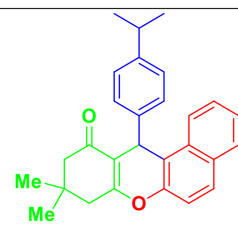 4	84/10	4.2	0.42	(160 – 164)	(160–162)[59]

m, Ar–H). ^{13}C NMR (75 MHz, $CDCl_3$): δ (ppm) 27.1, 29.3, 32.2, 34.7, 41.4, 50.9, 114.3, 117.0, 117.7, 123.7, 124.9, 126.2, 127.0, 128.2, 128.4. 128.4, 128.8, 131.4, 131.5, 144.7, 147.7, 163.9, 196.9. MS (70 eV, EI), m/z (%) 354 (M^+), 340 (M^+–O), 324 ($M^+–C_2H_6$), 277 ($M^+–C_6H_5$).

12-(4-Isopropylphenyl)-9,9-dimethyl-8,9,10,12-tetrahydro-11H-benzo[a]xanthen-11-one (4)

Yield = 84%, ^1H NMR (300 Hz, $CDCl_3$): δ (ppm) 1.02 (3H, s, CH_3), 1.15 (6H, d, CH_3) 1.17 (3H, s, CH_3) 2.31 (2H, s, CH_2), 2.61 (2H, CH_2), 2.72–2.83 (1H, m, CH), 5.71 (1H, s, CH), 7.03–8.08 (10H, m, Ar–H). ^{13}C NMR (75 MHz, $CDCl_3$): δ (ppm) 23.8, 27.4, 29.2, 30.9, 33.5, 41.4, 50.9, 110.1, 117.1, 121.3, 122.2, 123.8, 124.8, 126.2, 126.9, 127.3, 128.1, 128.3, 128.6, 131.4, 146.4, 157.2, 163.8, 197. MS (70 eV, EI), *m/z* (%) 396 (M^+), 382 (M^+–O), 277 ($M^+–C_6H_{11}$).

General procedure for the synthesis of 14–aryl–14H–dibenzo[a,j]xanthenes derivatives:

A mixture of aromatic aldehyde (1.0 mmol), 2 – naphthol (2.0 mmol), and Fe_3O_4@Agar-Ag NPs (20 mmol%) in EtOH (2 mL) was stirred in an oil bath at reflux conditions. The progress of the reaction was monitored by TLC, and after the completion of the reaction, the catalyst was separated from the mixture using an external magnet. The resulting solid was filtered off and recrystallized by ethanol.

Synthesis of 14-(p- tolyl)-14H-dibenzo[a,j]xanthene (11)

Yield = 90%, ^1H NMR (300 Hz, $CDCl_3$): δ (ppm) 2.17 (3H, d, CH_3), 6.50 (1H, s, CH), 6.98–7.00 (2H, d, CH), 7.41–7.53 (6H, m, CH), 7.59–7.64 (3H, t, CH), 7.81–7.87(4H, m, CH), 8.42–8.45 (2H, d, CH). ^{13}C NMR (75 MHz, $CDCl_3$): δ (ppm)

Table 2 (continued)

5	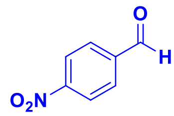	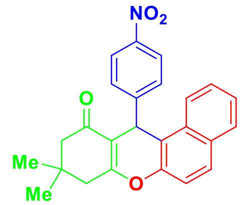 **5**	95/6	4.75	0.79	(173 – 177)	(175–177)[60]
6	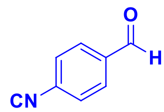	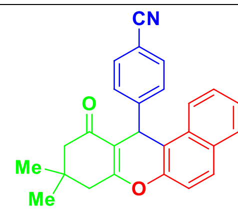 **6**	89/8	4.45	0.55	(200 – 203)	(201–203)[61]
7	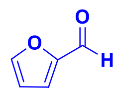	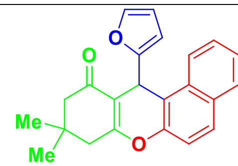 **7**	80/10	4	0.4	(169 – 173)	(170 – 172)[62]
8	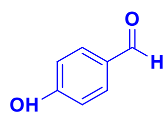	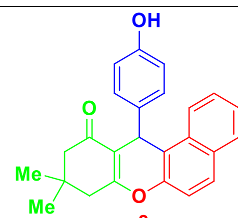 **8**	80/10	4	0.4	(220 – 222)	(218–220)[60]
9	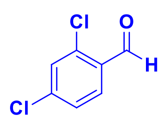	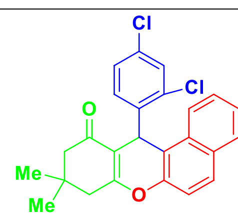 **9**	84/9	4.2	0.46	(174 – 177)	(176 – 177)[62]

20.8, 37.6, 117.4, 118.0, 122.7, 124.2, 126.7, 128.1, 128.7, 128.7, 129.1, 131.1, 131.4, 135.9, 142.1, 148.7. MS (70 eV, EI), *m/z* (%) 372 (M^+), 357 (M^+–CH_3), 281 (M^+–C_7H_7).

General procedure for the synthesis of 1, 8−dioxo−octahydroxanthenes derivatives

A mixture of aromatic aldehyde (1.0 mmol), 5,5-dimethyl-1,3-cyclohexanedione (2 mmol), and Fe_3O_4@Agar-Ag NPs (20 mmol%) in EtOH (2 mL) was stirred in an oil bath at reflux. The progress of the reaction was monitored by TLC, and after the completion of the reaction, the catalyst extracts from the mixture using an external magnet. Then, the catalyst was washed several times with ethyl acetate/ethanol, and dried in a vacuum desiccator to reuse for the next reaction. The resulting solid was filtered off and recrystallized by ethanol.

3,3,6,6-Tetramethyl-9-phenyl-3,4,5,6,7,9-hexahydro-1H-xanthene-1,8(2H)-dione (14)

Yield = 96%, ^{1}H NMR (300 Hz, $CDCl_3$): δ (ppm) 1.08 (6H, s, CH_3), 1.27 (6H, s, CH_3), 2.38- 2.50 (8H, m, CH_2), 5.59 (1H, s, CH), 7.12–7.33 (5H, m, Ar–H). ^{13}C NMR (75 MHz, $CDCl_3$): δ (ppm) 27.3, 27.4, 29.3, 29.6, 29.3, 29.6, 31.4, 32.2, 32.7, 40.8, 46.5, 47.1, 50.7, 115.5, 125.8, 126.3, 126.8, 128.1, 128.2, 128.4, 138.1, 144.1, 162.3, 189.4, 190.5. MS (70 eV, EI), *m/z* (%) 350 (M^+), 273 (M^+–C_6H_5).

Table 2 (continued)

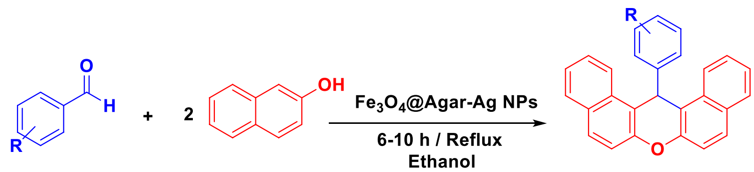

Entry	Aldehyde	Product	Yield (%) / Time(h)	TON	TOF (h^{-1})	Mp (found) °C	Mp (Lit.) °C
10	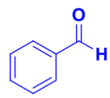	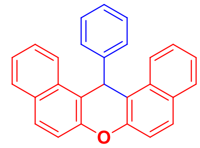 10	94/6	4.7	0.78	(178 – 182)	(183)[63]
11	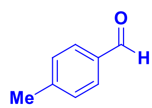	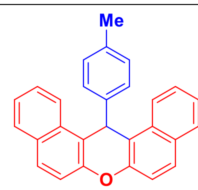 11	90/10	4.5	0.45	(220–223)	(228)[63]
12	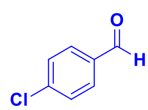	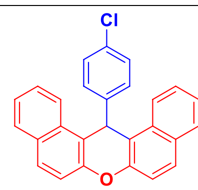 12	91/8	4.55	0.56	(285–288)	(287)[63]
13	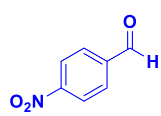	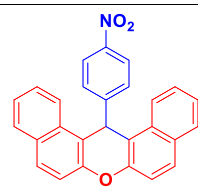 13	93/6	4.65	0.77	(310–313)	(312)[63]

Table 2 (continued)

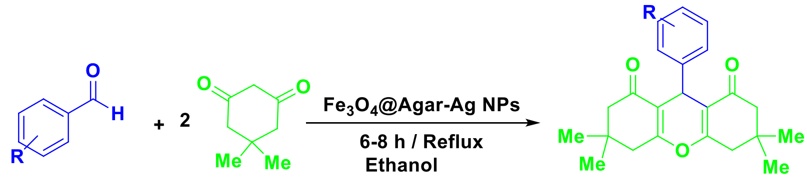

Entry	Aldehyde	Product	Yield (%) /Time(h)	TON	TOF (h^{-1})	Mp (found) °C	Mp (Lit.) °C
14	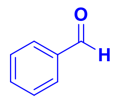	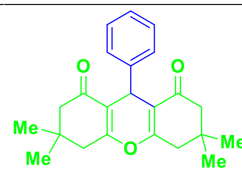 **14**	96/6	4.8	0.80	(201–204)	(205–207)[64]
15	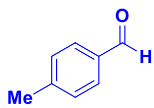	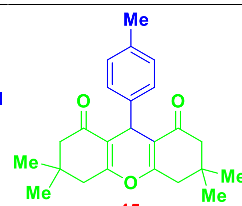 **15**	89/7	4.45	0.63	(217–220)	(218–220)[64]
16	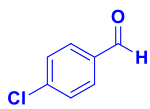	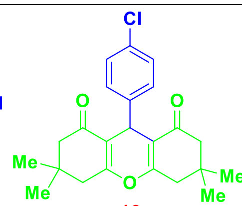 **16**	83/8	4.15	0.51	(229–234)	(230–232)[64]
17	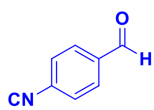	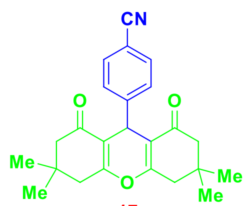 **17**	84/10	4.2	0.42	(250–253)	(251–253)[65]

Table 2 (continued)

18	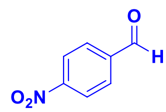	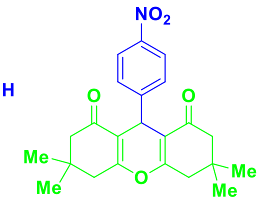 **18**	93/6	4.65	0.77	(220–224)	(221 – 223)[64]
19	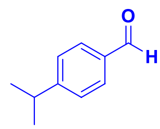	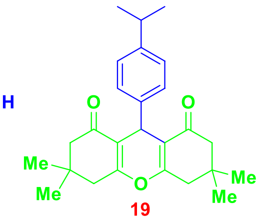 **19**	88/7	4.4	0.62	(170–174)	(170–172)[66]
20	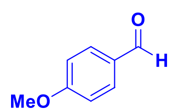	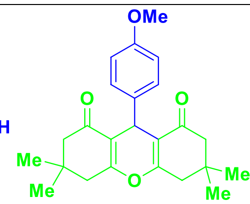 **20**	90/7	4.5	0.64	(240–242)	(241–243)[67]

Reaction conditions: Aldehyde (1 mmol), dimedone (2 mmol), Ethanol (96%) (2 ml), nanocatalyst (20 mmol%), Temperature reflux condition, Time 6-8 h.

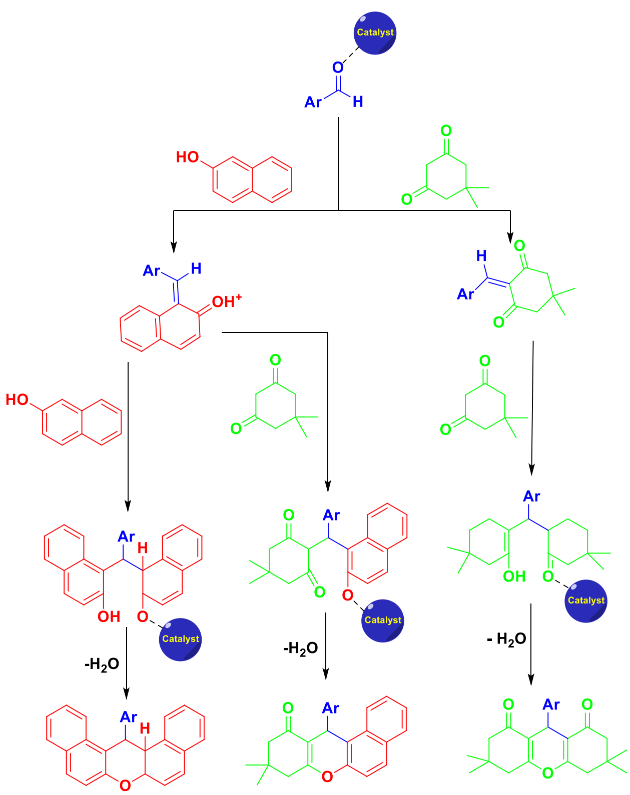

Fig.9 The possible mechanism for the synthesis of xanthenes

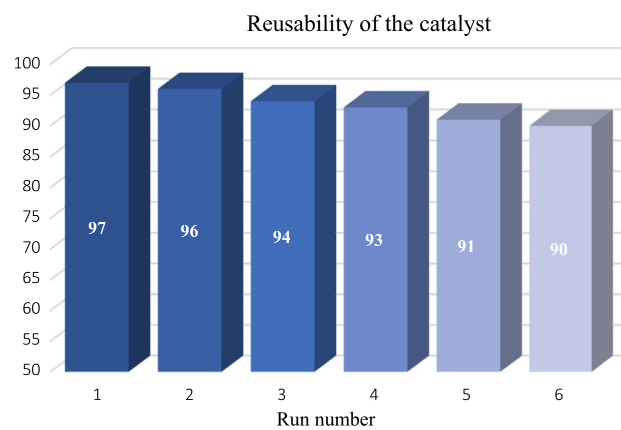

Fig.10 Reusability of the catalyst for the main reaction

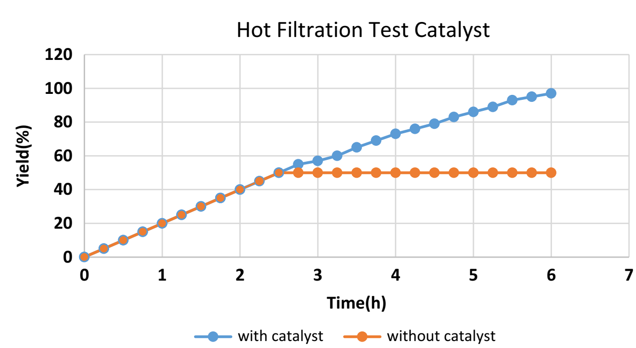

Fig.11 Hot filtration test of the Fe_3O_4@Agar-Ag NPs

Table 3 The comparison of Fe_3O_4@Agar-Ag NPs for the synthesis of xanthene derivatives with other reported ones in literature

Entry	Condition	Time	Yield (%)	Ref
1	[TEASA][TFA] (15 mol%)-100 °C, Solvent-free	10 m	80	[18]
2	$H_5PW_{10}V_2O_{40}$/MCM-48, Solvent-free—100 °C	6 h	95	[16]
3	$HClO_4$–SiO_2 and PPA–SiO_2 Acetonitrile Reflux	6 h	54	[17]
4	Fe_3O_4@Agar-Ag NPs-Ethanol—Reflux	6-10 h	80–96	Current Work

Supplementary Information The online version contains supplementary material available at https://doi.org/10.1007/s11030-021-10368-3.

Acknowledgements The authors gratefully acknowledge the Research Council of Ferdowsi University of Mashhad (3/52357).

References

1. Maleki A, Aghaei M, Ghamari N (2016) Facile synthesis of tetrahydrobenzoxanthenones via a one-pot three-component reaction using an eco-friendly and magnetized biopolymer chitosan-based heterogeneous nanocatalyst. Appl Organomet Chem 30:939–942. https://doi.org/10.1002/aoc.3524
2. Tabatabaeian K, Khorshidi A, Mamaghani M et al (2011) One-pot synthesis of tetrahydrobenzo[a]xanthen-11-one derivatives catalyzed by ruthenium chloride hydrate as a homogeneous catalyst. Can J Chem 89:623–627. https://doi.org/10.1139/v11-042
3. Shirini F, Khaligh NG (2012) Succinimide-N-sulfonic acid: an efficient catalyst for the synthesis of xanthene derivatives under solvent-free conditions. Dye Pigment 95:789–794. https://doi.org/10.1016/j.dyepig.2012.06.022
4. Kumar A, Rout L, Achary LSK et al (2017) Greener route for synthesis of aryl and alkyl-14H-dibenzo [a.j] xanthenes using graphene oxide-copper ferrite nanocomposite as a recyclable heterogeneous catalyst. Sci Rep. https://doi.org/10.1038/srep42975
5. Rahimi J, Maleki A (2020) Preparation of a trihydrazinotriazine-functionalized core-shell nanocatalyst as an extremely efficient catalyst for the synthesis of benzoxanthenes. Mater Today Chem 18:100362. https://doi.org/10.1016/j.mtchem.2020.100362
6. Bacci JP, Kearney AM, Van Vranken DL (2005) Efficient two-step synthesis of 9-aryl-6-hydroxy-3H-xanthen-3-one fluorophores. J Org Chem 70:9051–9053. https://doi.org/10.1021/jo051243i
7. Naidu KRM, Krishna BS, Kumar MA et al (2012) Design, synthesis and antiviral potential of 14-aryl/heteroaryl-14H- dibenzo[a, j]xanthenes using an efficient polymer-supported catalyst. Molecules 17:7543–7555. https://doi.org/10.3390/molecules17067543
8. Dos Santos WH, Da Silva-Filho LC (2016) Facile and efficient synthesis of xanthenedione derivatives promoted by niobium pentachloride. Chem Pap 70:1658–1664. https://doi.org/10.1515/chempap-2016-0098
9. El-Brashy AM, El-Sayed Metwally M, El-Sepai FA (2004) Spectrophotometric determination of some fluoroquinolone antibacterials by binary complex formation with xanthene dyes. Farmaco 59:809–817. https://doi.org/10.1016/j.farmac.2004.07.001
10. Knight CG, Stephens T (1989) Xanthene-dye-labelled phosphatidylethanolamines as probes of interfacial pH. Stud Phospholipid Vesicles Biochem J 258:683–689. https://doi.org/10.1042/bj2580683
11. Rewcastle GW, Atwell GJ, Zhuang L et al (1991) Potential antitumor agents. 61. structure-activity relationships for in vivo colon 38 activity among disubstituted 9-Oxo-9H-xanthene-4-acetic Acids. J Med Chem 34:217–222. https://doi.org/10.1021/jm00105a034
12. Jung H-A, Su B-N, Keller WJ et al (2006) Antioxidant xanthones from the pericarp of garcinia mangostana (Mangosteen). J Agric Food Chem 54:2077–2082. https://doi.org/10.1021/jf052649z
13. Makino M, Fujimoto Y (1999) Flavanones from Baeckea frutescens. Phytochemistry 50:273–277. https://doi.org/10.1016/S0031-9422(98)00534-2
14. Hiranrat A, Mahabusarakam W (2008) New acylphloroglucinols from the leaves of Rhodomyrtus tomentosa. Tetrahedron 64:11193–11197. https://doi.org/10.1016/j.tet.2008.09.054
15. E-journal CE, Hassankhani A, Mosaddegh E et al (2012) H4SiW12O40 catalyzed one-pot synthesis of 12-aryl-8,9,10,12-tetrahydrobenzo[a]xanthen-11-ones under solvent free conditions. 9:786–790
16. Reza Tayebee BM (2017) diazepine - tetrazole and benzodiazepine - 2 - carboxamide derivatives with the aid of MCM - 48 / H 5 PW 10 V 2 O 40. J Chem Sci 125:335–344
17. Kantevari S, Bantu R, Nagarapu L (2007) HClO4-SiO2 and PPA-SiO2 catalyzed efficient one-pot Knoevenagel condensation, Michael addition and cyclo-dehydration of dimedone and aldehydes in acetonitrile, aqueous and solvent free conditions: scope and limitations. J Mol Catal A Chem 269:53–57. https://doi.org/10.1016/j.molcata.2006.12.039
18. Saadat A, Zare A, Jamadi F, Abdolalipour-Saretoli M (2018) Highly efficient synthesis of 1-Thioamidoalkyl-2-naphthols and 14-Aryl-14H-dibenzo[a, j]xanthenes using a novel ionic liquid: Catalyst preparation, characterization and performing the reactions. Bull Chem React Eng & Catal 13:204–212. https://doi.org/10.9767/bcrec.13.2.1280.204-212
19. Sheikh S, Nasseri MA, Chahkandi M et al (2020) Functionalized magnetic PAMAM dendrimer as an efficient nanocatalyst for a new synthetic strategy of xanthene pigments. Hazard Mater 400: 122985.https://doi.org/10.1016/j.jhazmat.2020.122985
20. Venu Madhav J, Thirupathi Reddy Y, Narsimha Reddy P et al (2009) Cellulose sulfuric acid: an efficient biodegradable and recyclable solid acid catalyst for the one-pot synthesis of aryl-14H-dibenzo[a.j]xanthenes under solvent-free conditions. J Mol Catal A Chem 304:85–87. https://doi.org/10.1016/j.molcata.2009.01.028
21. Rezayati S, Erfani Z, Hajinasiri R (2015) Phospho sulfonic acid as efficient heterogeneous Brønsted acidic catalyst for one-pot synthesis of 14H-dibenzo[a, j]xanthenes and 1,8-dioxo-octahydroxanthenes. Chem Pap 69:536–543. https://doi.org/10.1515/chempap-2015-0058
22. Maleki A (2012) Fe 3O 4/SiO 2 nanoparticles: an efficient and magnetically recoverable nanocatalyst for the one-pot multicomponent synthesis of diazepines. Tetrahedron 68:7827–7833. https://doi.org/10.1016/j.tet.2012.07.034
23. Maleki A (2013) One-pot multicomponent synthesis of diazepine derivatives using terminal alkynes in the presence of silica-supported superparamagnetic iron oxide nanoparticles. Tetrahedron Lett 54:2055–2059. https://doi.org/10.1016/j.tetlet.2013.01.123
24. Maleki A (2014) One-pot three-component synthesis of pyrido[2′,1′:2,3]imidazo[4,5-c]isoquinolines using Fe3O4@

SiO2-OSO3H as an efficient heterogeneous nanocatalyst. RSC Adv 4:64169–64173. https://doi.org/10.1039/c4ra10856f
25. Maleki A (2018) Green oxidation protocol: selective conversions of alcohols and alkenes to aldehydes, ketones and epoxides by using a new multiwall carbon nanotube-based hybrid nanocatalyst via ultrasound irradiation. Ultrason Sonochem 40:460–464. https://doi.org/10.1016/j.ultsonch.2017.07.020
26. Esmaeili MS, Varzi Z, Taheri-Ledari R, Maleki A (2021) Preparation and study of the catalytic application in the synthesis of xanthenedione pharmaceuticals of a hybrid nano-system based on copper, zinc and iron nanoparticles. Res Chem Intermed 47:973–996. https://doi.org/10.1007/s11164-020-04311-8
27. Trang VT, Tam LT, Van Quy N et al (2017) Functional iron oxide-silver hetero-nanocomposites: controlled synthesis and antibacterial activity. J Electron Mater 46:3381–3389. https://doi.org/10.1007/s11664-017-5314-2
28. Mousavi Mashhadi SA, Kassaee MZ, Eidi E (2019) Magnetically recyclable nano copper/chitosan in O-arylation of phenols with aryl halides. Appl Organomet Chem 33:1–7. https://doi.org/10.1002/aoc.5042
29. Ghavami M, Koohi M, Kassaee MZ (2013) Selective nanocatalyst for an efficient Ugi reaction: magnetically recoverable Cu(acac)2/NH2-T/SiO2atFe3O4 nanoparticles. J Chem Sci 125:1347–1357. https://doi.org/10.1007/s12039-013-0506-7
30. Abdolmohammadi S, Hossaini Z (2019) Fe3O4 MNPs as a green catalyst for syntheses of functionalized [1,3]-oxazole and 1H-pyrrolo-[1,3]-oxazole derivatives and evaluation of their antioxidant activity. Mol Divers 23:885–896. https://doi.org/10.1007/s11030-019-09916-9
31. Chen Y, Zhang Z, Jiang W et al (2019) RuIII@CMC/Fe3O4 hybrid: an efficient, magnetic, retrievable, self-organized nanocatalyst for green synthesis of pyranopyrazole and polyhydroquinoline derivatives. Mol Divers 23:421–442. https://doi.org/10.1007/s11030-018-9887-3
32. Ezzatzadeh E (2021) Chemoselective oxidation of sulfi des to sulfoxides using a novel Zn-DABCO functionalized Fe3O4 MNPs as highly effective nanomagnetic catalyst. Asian J Nanosci Mater 4:125–136. https://doi.org/10.26655/AJNANOMAT.2021.2.3
33. Ezzatzadeh E, Hossaini Z (2020) 2D ZnO/Fe3O4 nanocomposites as a novel catalyst-promoted green synthesis of novel quinazoline phosphonate derivatives. Appl Organomet Chem 34:e5596. https://doi.org/10.1002/aoc.5596
34. Rezayati S, Ramazani A, Sajjadifar S et al (2021) Design of a schiff base complex of copper coated on epoxy-modified core-shell MNPs as an environmentally friendly and novel catalyst for the one-pot synthesis of various chromene-annulated heterocycles. ACS Omega 6:25608–25622. https://doi.org/10.1021/acsomega.1c03672
35. Wang M, Han J, Shi H (2020) Synthesis and inhibition performance of a Fe3O4/Chitosan-supported inhibitor. J Vinyl Addit Technol 26:304–308. https://doi.org/10.1002/vnl.21744
36. Nian D, Shi P, Sun J et al (2019) Application of luteinizing hormone-releasing hormone–ferrosoferric oxide nanoparticles in targeted imaging of breast tumors. J Int Med Res 47:1749–1757. https://doi.org/10.1177/0300060519834457
37. Sadjadi S, Kahangi FG, Dorraj M, Heravi MM (2020) Ag nanoparticles stabilized on cyclodextrin polymer decorated with multi-nitrogen atom containing polymer: an efficient catalyst for the synthesis of xanthenes. Molecules. https://doi.org/10.3390/molecules25020241
38. Maleki A, Panahzadeh M, Eivazzadeh-keihan R (2019) Agar: a natural and environmentally-friendly support composed of copper oxide nanoparticles for the green synthesis of 1,2,3–triazoles. Green Chem Lett Rev 12:395–406. https://doi.org/10.1080/17518253.2019.1679263
39. Bahrami S, Hassanzadeh-Afruzi F, Maleki A (2020) Synthesis and characterization of a novel and green rod-like magnetic ZnS/CuFe2O4/agar organometallic hybrid catalyst for the synthesis of biologically-active 2-amino-tetrahydro-4H-chromene-3-carbonitrile derivatives. Appl Organomet Chem 34:1–15. https://doi.org/10.1002/aoc.5949
40. Eivazzadeh-Keihan R, Moghim Aliabadi HA, Radinekiyan F et al (2021) Investigation of the biological activity, mechanical properties and wound healing application of a novel scaffold based on lignin-agarose hydrogel and silk fibroin embedded zinc chromite nanoparticles. RSC Adv 11:17914–17923. https://doi.org/10.1039/d1ra01300a
41. Xiao Q, Liu C, Ni H et al (2019) β-Agarase immobilized on tannic acid-modified Fe3O4 nanoparticles for efficient preparation of bioactive neoagaro-oligosaccharide. Food Chem 272:586–595. https://doi.org/10.1016/j.foodchem.2018.08.017
42. Armisén R, Gaiatas F (2009) Agar. In: Phillips GO, Williams PA (eds) Handbook of hydrocolloids. Woodhead Publishing Limited, pp 82–107. https://doi.org/10.1533/9781845695873.82.
43. Hsieh SL, Huang BY, Hsieh SL et al (2010) Green fabrication of agar-conjugated Fe3O4 magnetic nanoparticles. Nanotechnology. https://doi.org/10.1088/0957-4484/21/44/445601
44. Hoseinzade K, Mousavi-Mashhadi SA, Shiri A (2021) Copper immobilization on Fe_3O_4@Agar: an efficient superparamagnetic nanocatalyst for green ullmann-type cross-coupling reaction of primary and secondary amines with aryl iodide derivatives. J Inorg Organomet Polym Mater 31:4648–4658. https://doi.org/10.1007/s10904-021-02106-x
45. Sonei S, Gholizadeh M, Taghavi F (2020) Cu(II) anchored on modified magnetic nanoparticles: as a green and efficient recyclable nano catalyst for one pot synthesis of 12-Aryl-8,9,10,12tetrahydrobenzo[a]xanthene-11-one″. Polycycl Aromat Compd 40:1127–1142. https://doi.org/10.1080/10406638.2018.1531431
46. Skumiel A, Kaczmarek K, Flak D et al (2020) The influence of magnetic nanoparticle concentration with dextran polymers in agar gel on heating efficiency in magnetic hyperthermia. J Mol Liq. https://doi.org/10.1016/j.molliq.2020.112734
47. Dung TT, Danh TM, Hoa LTM et al (2009) Structural and magnetic properties of starch-coated magnetite nanoparticles. J Exp Nanosci 4:259–267. https://doi.org/10.1080/17458080802570609
48. Gecim B, Winer WO (1987) Thermal conductivity of lubricants at high pressures. J Tribol 109:566–567. https://doi.org/10.1115/1.3261507
49. Burduşel AC, Gherasim O, Grumezescu AM et al (2018) Biomedical applications of silver nanoparticles: an up-to-date overview. Nanomaterials 8:1–24. https://doi.org/10.3390/nano8090681
50. Keyhaniyan M, Shiri A, Eshghi H, Khojastehnezhad A (2018) Novel design of recyclable copper(II) complex supported on magnetic nanoparticles as active catalyst for Beckmann rearrangement in poly(ethylene glycol). Appl Organomet Chem 32:1–10. https://doi.org/10.1002/aoc.4344
51. Ghadamyari Z, Shiri A, Khojastehnezhad A, Seyedi SM (2019) Zirconium (IV) porphyrin graphene oxide: a new and efficient catalyst for the synthesis of 3,4-dihydropyrimidin-2(1H)-ones. Appl Organomet Chem 33:1–10. https://doi.org/10.1002/aoc.5091
52. Keyhaniyan M, Shiri A, Eshghi H, Khojastehnezhad A (2018) Synthesis, characterization and first application of covalently immobilized nickel-porphyrin on graphene oxide for Suzuki cross-coupling reaction. New J Chem 42:19433–19441. https://doi.org/10.1039/c8nj04157a
53. Ghadamyari Z, Khojastehnezhad A, Seyedi SM, Shiri A (2019) Co(II)-porphyrin immobilized on graphene oxide: an efficient catalyst for the beckmann rearrangement. ChemistrySelect 4:10920–10927. https://doi.org/10.1002/slct.201902811

54. Rafiee E, Ataei A, Nadri S et al (2014) Combination of palladium and oleic acid coated-magnetite particles: characterization and using in Heck coupling reaction with magnetic recyclability. Inorganica Chim Acta 409:302–309. https://doi.org/10.1016/j.ica.2013.09.042
55. Mousavi M, Bakavoli M, Shiri A, Eshghi H (2018) Pure water-induced dehalogenation of 2,4-Di- tert-amino-6-substituted-5-halogenopyrimidines. ACS Sustain Chem Eng 6:5852–5857. https://doi.org/10.1021/acssuschemeng.7b04127
56. Mousavi-mashhadi SA, Shiri A (2021) On-water and efficient ullmann-type O-arylation cross coupling reaction of phenols and aryl tosylates in the presence of Fe_3O_4@Starch-Au as Nanocatalyst. Chemistry Select 6:3941–3951. https://doi.org/10.1002/slct.202004327
57. Esfahani HRM, Foroughifar N, Mobinikhaledi A, Moghanian H (2013) Ammonium oxalate as an efficient catalyst for one-pot synthesis of tetrahydrobenzo [a]xanthen-11-one derivatives under solvent-free conditions. Synth React Inorg Met Nano-Metal Chem 43:752–755. https://doi.org/10.1080/15533174.2012.754767
58. Bi Fatemeh Mirjalili B, Bamoniri A, Zamani L (2012) Nano-$TiCl_4/SiO_2$: an efficient and reusable catalyst for the synthesis of tetrahydrobenzo[a]xanthenes-11-ones. Lett Org Chem 9:338–343. https://doi.org/10.2174/157017812801264700
59. Zare Fekri L, Darya-Laal AR (2020) NiFe2O4@SiO2@amino glucose magnetic nanoparticle as a green, effective and magnetically separable catalyst for the synthesis of xanthene-ones under solvent-free condition. Polycycl Aromat Compd 40:1539–1556. https://doi.org/10.1080/10406638.2018.1559207
60. Taghavi F, Gholizadeh M, Saljooghi AS, Ramezani M (2016) Metal free synthesis of tetrahydrobenzo[: A] xanthenes using orange peel as a natural and low cost efficient heterogeneous catalyst. RSC Adv 6:87082–87087. https://doi.org/10.1039/c6ra17607k
61. Mane P, Shinde B, Mundada P et al (2020) Sodium acetate/MWI: a green protocol for the synthesis of tetrahydrobenzo[α]xanthen-11-ones with biological screening. Res Chem Intermed 46:231–241. https://doi.org/10.1007/s11164-019-03945-7
62. Rajitha B, Sunil Kumar B, Thirupathi Reddy Y et al (2005) Sulfamic acid: a novel and efficient catalyst for the synthesis of aryl-14H-dibenzo[a.j]xanthenes under conventional heating and microwave irradiation. Tetrahedron Lett 46:8691–8693. https://doi.org/10.1016/j.tetlet.2005.10.057
63. Thirumalai D, Gajalakshmi S (2020) An efficient heterogeneous iron oxide nanoparticle catalyst for the synthesis of 9-substituted xanthene-1,8-dione. Res Chem Intermed 46:2657–2668. https://doi.org/10.1007/s11164-020-04112-z
64. Hasaninejad A, Shekouhy M, Miar M, Firoozi S (2016) Sulfonated polyethylene glycol (PEG-SO3H) as eco-friendly and potent water soluble solid acid for facile and green synthesis of 1,8-Dioxo-Octahydroxanthene and 1,8-Dioxo-Decahydroacridine derivatives. Synth React Inorg Met Nano-Metal Chem 46:151–157. https://doi.org/10.1080/15533174.2014.900799
65. Chaudhary GR, Bansal P, Kaur N, Mehta SK (2014) Recyclable CuO nanoparticles as heterogeneous catalysts for the synthesis of xanthenes under solvent free conditions. RSC Adv 4:49462–49470. https://doi.org/10.1039/c4ra07620f
66. Zhou J, Liu D, Wu F et al (2019) Synthesis of SCMNPs@imine/SO3H magnetic nanocatalyst by chlorosulfonic acid as sulfonating agents and their application for the preparation of 12-aryl-8,9,10,12-tetrahydrobenzo[a]xanthen-11-one and 1,8-dioxooctahydroxanthene derivatives. Mater Res Exp. https://doi.org/10.1088/2053-1591/ab5c90

Authors and Affiliations

Kimia Hoseinzade[1] · Seyed Ali Mousavi-Mashhadi[1] · Ali Shiri[1]

✉ Ali Shiri
alishiri@um.ac.ir

[1] Department of Chemistry, Faculty of Science, Ferdowsi University of Mashhad, Mashhad, Iran